

FLATNESS-BASED CONTROL OF FLEXIBLE MOTION SYSTEMS

Brian K. Post *

Intelligent Machine Dynamics Laboratory
George Woodruff School of Mechanical Engineering
Georgia Institute of Technology
Atlanta, Georgia 30332
bkpost@gatech.edu

Alexandre Mariuzza

George Woodruff School of Mechanical Engineering
Georgia Institute of Technology
Atlanta, Georgia 30332
amariuzza3@gatech.edu

Wayne J. Book

Intelligent Machine Dynamics Laboratory
George Woodruff School of Mechanical Engineering
Georgia Institute of Technology
Atlanta, Georgia 30332
wayne.book@me.gatech.edu

William Singhose

Advanced Crane Control Laboratory
George Woodruff School of Mechanical Engineering
Georgia Institute of Technology
Atlanta, Georgia 30332
singhose@gatech.edu

ABSTRACT

Flexibility is often an unavoidable limitation when large-workspace high-speed manipulation is required. This flexibility can be mitigated in some circumstances through feedback control methods. However, these methods only correct for vibration after it has been measured. Therefore, if low-vibration reference commands can be generated, then the utility of these systems can be greatly improved. However, there are instances where system nonlinearities limit the effectiveness of many command-shaping techniques. This paper proposes a method for the generation of fast vibration-limiting trajectories for flexible systems based on the differential-flatness property of nonlinear systems. This approach is applied to a tower crane for simulation and experimental validation. The results are compared to those from standard command-shaping techniques. Practical implementation issues for real world systems are discussed.

INTRODUCTION

Flexible motion systems are prone to excessive and undesired vibration when operated near their performance limits. To mitigate these effects they are often operated well below their capable operating speeds. This not only limits the efficiency of

these systems, but also hinders their functionality, as dexterity, performance, and workspace size are sacrificed for accuracy and reliability.

While feedback control yields performance improvements in vibration reduction and the ability to correct for external disturbances, errors between desired and ideal behavior must be measured before any control action is applied. Therefore, potential control structures should utilize reference command trajectories that result in a low level of undesired and potentially damaging vibration. In doing so, the utility of these systems can be expanded and the burden on reactive feedback control can be reduced.

While many motion systems are human operated in real time, like most industrial cranes and excavators, a large number use preprogrammed or repeated trajectories. For example, industrial robots used in manufacturing are often programmed to repeatedly perform the same motion. In some cases the control objective is to track a desired trajectory, for obstacle avoidance or efficiency. In other cases it is primarily to complete a motion by ending in the desired location. In either case, it is useful if the trajectory results in a reduction of both residual vibration and transient deflection.

*Address all correspondence to this author.

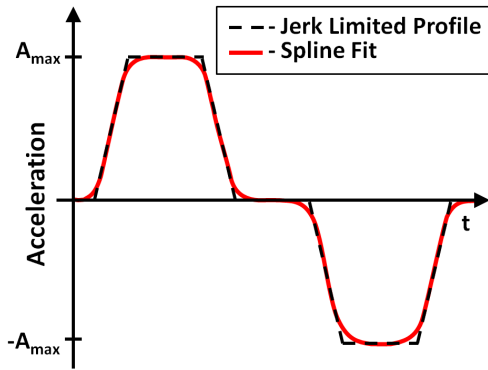


Figure 1. JERK LIMITED ACCELERATION PROFILE

We propose a method to generate trajectories for flexible motion systems with predetermined way-point targets. It is based on the differential flatness property of nonlinear systems as developed in [6] and generates paths that result in both a reduction in residual vibration and transient deflection while enabling high-speed operation. This method is then applied to a tower crane in simulations and experiments aimed at accessing the effectiveness of the command generation approach to provide fast, vibration-limiting motions. The results are benchmarked against common command-shaping techniques.

FLATNESS-BASED CONTROL

Differential Flatness as discussed in [4, 6, 7, 9, 13] is a property akin to controllability of linear systems. It ensures the existence of a transformation from the desired output to a controlled variable. Flatness based control, is one method of inverse dynamics [4, 10, 14, 21] where a “flat output” is used to develop this mapping between output and input. The existence of a flat output means that the state x and input u can be directly expressed in terms of the output y and a finite number of its derivatives without the solution of a differential equation as described by:

$$\begin{aligned} x &= A(y, \dot{y}, \ddot{y}, \dots) \\ u &= B(y, \dot{y}, \ddot{y}, \dots) \end{aligned} \quad (1)$$

Therefore, given a set of desired flat trajectories, command profiles can be directly determined that yield the desired output. As a result, if a flat trajectory is specified that has no oscillatory behavior, then the command produced by the mapping should result in no vibration. This, of course, relies on the assumption that every behavior of the dynamic system is modeled very accurately and that the system is capable of producing the command profiles.

This formulation produces additional constraints for the specification of the desired trajectories, most importantly that the trajectory must be continuous, at a minimum, to the highest order dynamic of the flat output. However, in the literature it is suggested that for a C^2 dynamic system the specified trajectory be at least C^4 [7]. Finally, at the initial and final position the successive derivatives must be zero, i.e. for a C^2 system

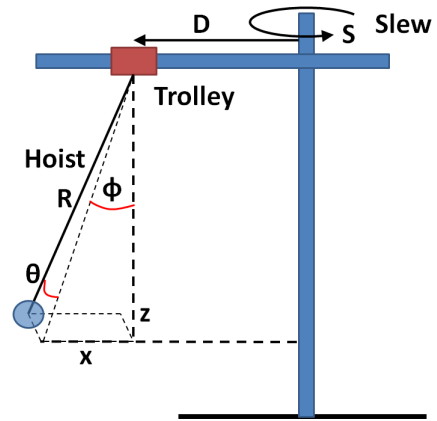


Figure 2. TOWER CRANE DIAGRAM

$\dot{y}(0), \ddot{y}(0), y^{(3)}(0), y^{(4)}(0) = 0$ and $\dot{y}(t_f), \ddot{y}(t_f), y^{(3)}(t_f), y^{(4)}(t_f) = 0$. To satisfy these constraints a polynomial is traditionally generated whose coefficients are matched to the specific boundary conditions [21]. However, this results in an S-curve like trajectory, which only reaches the maximum velocity at one instant in time. Thus, this approach can result in slow commands that hinder system performance [18].

Therefore, to define the trajectories used in this study, switching times for the acceleration profile of a jerk-limited command, described in [19], were calculated. Then, a third-order spline curve with the appropriate boundary conditions was fit to the desired acceleration to create a trajectory that satisfied all of the conditions for the flat output formulation. This process is shown in Figure 1. This curve was then numerically integrated with a simple trapezoidal approximation and a 1 millisecond sampling rate to determine the velocity profile, and integrated again to determine the position trajectory. Once the trajectory was completely defined, the flatness-based control algorithm was executed to produce the desired commands. These commands were then checked against the performance capabilities of the motors and drives. If the commands violated the velocity or acceleration limits, then the design trajectories were modified by selectively reducing the aggressiveness of the desired motions. This procedure was carried out iteratively until the commands produced were within the capabilities of the system.

TOWER CRANE MODELING

As illustrated in Figure 2, a tower crane consists of three controllable parameters, the suspension cable length R , the trolley radial position D and the slew angle S as described in [8]. Motion of these axes results in payload swing in the radial ϕ and tangential directions θ . Assuming the cable length changes slowly, the swing dynamics can be modeled by (2), as described in [3].

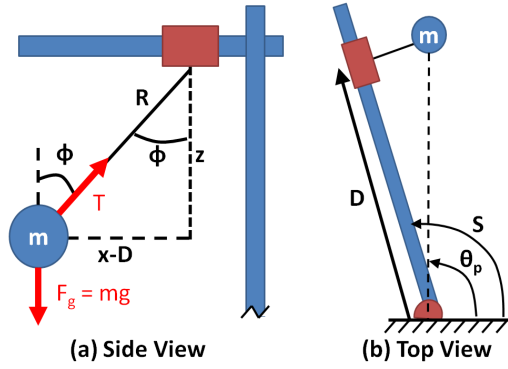


Figure 3. SIMPLIFIED SYSTEM DIAGRAMS

$$\begin{aligned}
 R\ddot{\phi} + R\dot{\theta} \cos(\phi) \sin(\phi) + g \cos(\theta) = \\
 -\ddot{D} \cos(\phi) + D\dot{S}^2 \cos(\phi) - D\dot{S} \sin(\phi) \sin(\theta) \\
 -2\dot{D}\dot{S} \sin(\phi) \sin(\theta) - 2R\dot{S}\dot{\theta} \cos^2(\phi) \cos(\theta) \\
 -R\dot{S} \sin(\theta) + R\dot{S}^2 \sin(\phi) \cos^2(\theta) \cos(\phi)
 \end{aligned} \quad (2)$$

$$\begin{aligned}
 R\ddot{\theta} \cos(\phi) - 2R\dot{\phi}\dot{\theta} \sin(\phi) + g \sin(\theta) = \\
 D\dot{S} \cos(\theta) + 2\dot{D}\dot{S} \cos(\theta) + 2R\dot{S}\dot{\phi} \cos(\phi) \cos(\theta) \\
 + R\dot{S} \sin(\phi) \cos(\theta) + L\dot{S}^2 \sin(\theta) \cos(\phi) \cos(\theta)
 \end{aligned} \quad (3)$$

These nonlinear equations of motion were used in the simulations, but the coupling between the swing angles ϕ and θ and axes commands R , D , and S prevent (2) and (3) from satisfying the conditions of a differentially-flat system. Therefore, they were not used to generate the command trajectories. Instead a simplified model was derived by selecting a more convenient set of outputs and neglecting Coriolis terms, in order to satisfy the differential-flatness constraints.

Flat Outputs

Let the radial position x , vertical position z and rotation about the slew axis θ_p of the payload as shown in Figures 3(a) and 3(b) be the flat outputs of the tower crane. Then from Figure 3(a) the following equations of motion and geometric relations can be determined.

$$m\ddot{z} = mg - T \cos(\phi) \quad (4)$$

$$m\ddot{x} - mx\dot{\theta}_p^2 = -T \sin(\phi) \quad (5)$$

$$\cos(\phi) = \frac{z}{R} \quad (6)$$

$$\sin(\phi) = \frac{x-D}{R} \quad (7)$$

Substituting (6) and (7) into (4) and (5) yields the trolley displacement:

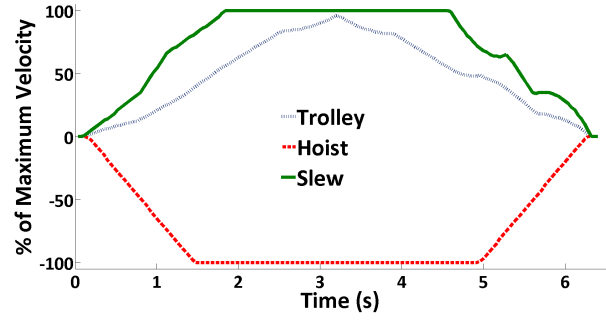


Figure 4. MOTION COMMANDS

$$D = x - \frac{z(\ddot{x} - x\dot{\theta}_p^2)}{\ddot{z} - g} \quad (8)$$

Assuming small tangential deflections, application of the Pythagorean theorem $R^2 = (x - D)^2 + z^2$ provides a solution for the cable length:

$$R^2 = z^2 + \left[\frac{z(\ddot{x} - x\dot{\theta}_p^2)}{\ddot{z} - g} \right]^2 \quad (9)$$

Treating the energy stored by gravity while the pendulum deviates from vertical, as illustrated in Figure 3(b), by a torsional spring with a spring constant of $K = \frac{mg}{R}$ yields the equation of motion:

$$S = \frac{R}{g} \ddot{\theta}_p + \theta_p \quad (10)$$

Note that the simplified crane model given in (8), (9), and (10) now satisfies the definition of a differentially flat system with flat outputs x , z , and θ_p . Therefore, by supplying the desired payload trajectory information at each time step (\ddot{x} , \dot{x} , x , \ddot{z} , z , $\ddot{\theta}_p$, $\dot{\theta}_p$, and θ_p) the necessary hoist length R , trolley position D , and slew angle S can be calculated in closed form. An example of those commands is shown in Figure 4.

It is also important to note that this formulation includes nonlinear coupling between the motion axes. This coupling appears in the form of centripetal acceleration from the motion of the slew axis, and changing natural frequency $\sqrt{\frac{g}{R}}$ from the changing hoist length. However, the coupling from Coriolis effects violates the differential-flatness constraints and was therefore neglected.

From this point on, this approach will be referred to as Crane Applied Inverse Dynamics (CAID). An illustration of the general control scheme is presented in Figure 5. Starting with a desired payload trajectory for each axis y_d , the CAID controller produces the commands necessary to achieve the desired motion. These

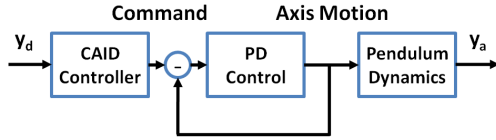


Figure 5. CONTROL STRUCTURE

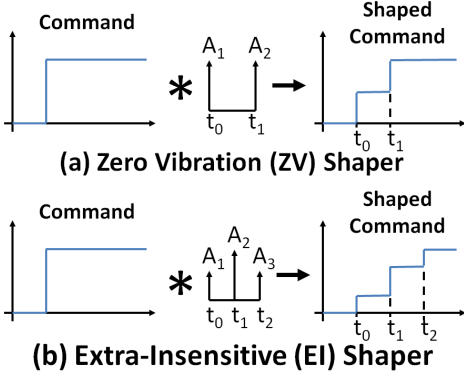


Figure 6. COMMAND SHAPERS

are then executed via PD feedback controllers for each motion axis. The result is a nearly direct one-to-one mapping between desired and actual payload trajectories.

SIMULATION

To examine the effectiveness of the proposed method for a tower crane, a simulation was performed using standard command shapers as benchmarks. For more thorough discussion of command-shaping techniques see [2, 3, 5, 11, 12, 15, 17, 19].

Command shaping seeks to reduce or eliminate residual vibration by generating a reference command that does not excite the oscillatory behavior of the system. Input shaping is a specific type of shaping that convolves the baseline command with a series of impulses. If the baseline command is a step input, then the shaped command will be a sequence of steps, as illustrated in Figure 6. The impulse times are directly related to the period of oscillation, and thus to the natural frequency of the system.

The zero vibration or ZV shaper as illustrated in the top part of Figure 6 is the simplest shaper. For undamped systems, it contains two equal impulses A_1 and A_2 separated by one half period of vibration [15, 20]:

$$\begin{bmatrix} A_i \\ t_i \end{bmatrix} = \begin{bmatrix} 0.5 & 0.5 \\ 0 & 0.5T \end{bmatrix} \quad (11)$$

As shown by the solid line in the top of Figure 7, the result is a move with no residual vibration and a time lag of $\frac{T}{2}$ relative to the unshaped (US) response.

While ideally resulting in zero vibration the ZV shaper is not robust to changes in the natural frequency of the system. Relaxing the vibration constraint at the design frequency to a tol-

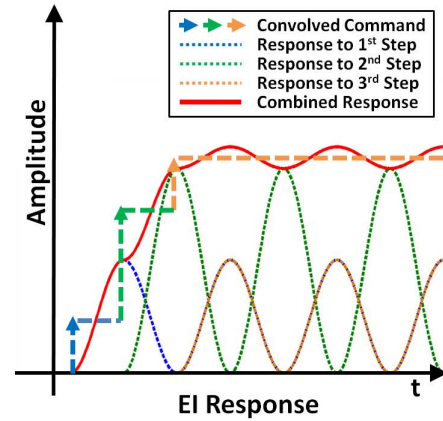
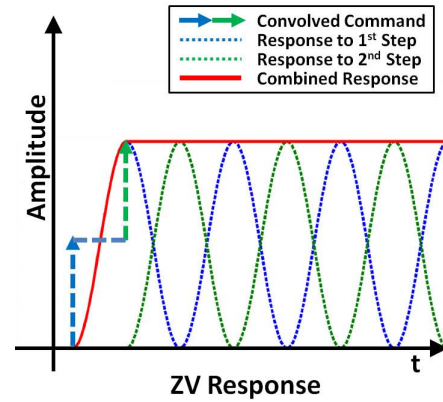


Figure 7. RESPONSES FOR UNDAMPED VIBRATORY SYSTEMS

erable level, V_{tol} , and adding another impulse to the shaper can significantly improve robustness. The resulting design is an extra insensitive (EI) shaper [16]:

$$\begin{bmatrix} A_i \\ t_i \end{bmatrix} = \begin{bmatrix} \frac{1+V_{tol}}{4} & \frac{1-V_{tol}}{2} & \frac{1+V_{tol}}{4} \\ 0 & 0.5T & T \end{bmatrix} \quad (12)$$

The increased robustness of the EI shaper comes at the expense of risetime that is increased by an additional half period, as seen in the lower part of Figure 7.

Figure 8 is a result of a simulation of the payload response to a 0.21m point-to-point motion of the trolley using all four control methodologies: unshaped (US), ZV shaped, EI shaped and with the CAID controller. It is immediately obvious that the ZV shaper, EI shaper, and CAID controller result in a drastic reduction in residual vibration of the payload when compared to the unshaped (trapezoidal velocity profile) case.

The move time, residual vibration, and the transient deflection are summarized in Table 1. These results show that for motion in the trolley axis with constant hoist length (1m), the ZV shaper and CAID controller perform the desired move in relatively comparable times, with the CAID controller slightly slower because the commands are moderately less aggressive. The EI shaper produces a significantly slower response.

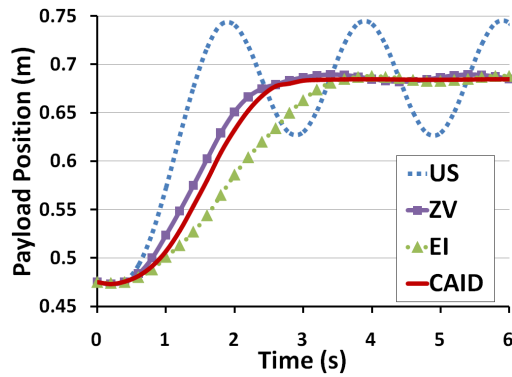


Figure 8. PAYLOAD RESPONSE

Table 1. TROLLEY POINT-TO-POINT RESPONSE

	US	ZV	EI	CAID
<i>Time (s)</i>	1.64	2.68	3.72	2.92
<i>Res. Vib (°)</i>	3.511	0.223	0.155	0.016
<i>Move Def. (°)</i>	2.732	1.195	0.626	0.754

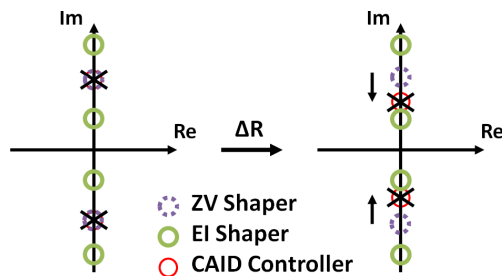


Figure 9. NONLINEAR EFFECTS

Also important to note is that while the ZV and EI shapers enforce conditions on the residual vibration, no direct attempt is made to minimize the payload sway during the move. In contrast, by specifying the position, velocity, and acceleration of the payload at every time step, the CAID controller results in less deflection during the move than the ZV shaper and faster move time than the EI shaper. The EI shaper does produce the lowest transient deflection, but at the cost of a 27% increase in execution time.

While comparable to the ZV shaper in both speed and residual vibration for the single axis case, the benefit of the CAID method becomes more noticeable as the nonlinearities of the system are amplified by slewing and changing the hoist length.

As illustrated by Figure 9, the overall effect of these methods is to place zeros in the vicinity of the flexible system poles reducing their effect in the response [1, 19]. The EI Shaper places a set of zeros above and below the vibratory poles resulting in a reduc-

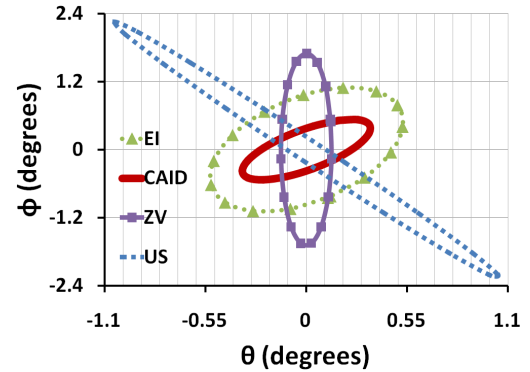


Figure 10. RESIDUAL VIBRATION PROFILES

tion of vibration for wide variations in natural frequency. However, the ZV shaper and CAID controller place zeros directly over the poles, effectively eliminating the oscillatory nature of the response, when the model is perfect. As the pole locations change, moving towards the real axis for increasing and away for decreasing hoist length, the ZV zero locations remain fixed, resulting in imperfect cancellation. The CAID zeros, however, attempt to track the changing poles.

Figure 10 shows the residual oscillation of the payload for a 0.53m trolley move, a 1.22m change in hoist length, and a 180 degree change in slew. The residual vibration in the radial direction is significantly lower with the CAID controller than either the ZV or EI shapers. In the tangential direction, the ZV shaper provides the smallest residual vibration. However, the magnitude of the residual vibration, as expressed by the norm of the maximum tangential and radial deflections, is significantly smaller for the CAID method.

EXPERIMENTS

The CAID method was tested on the portable tower crane shown in Figure 11. The experiments examined the practicality, performance, and robustness of the algorithm on a physical system with realistic performance limitations. Each axis of the crane was actuated via an AC servomotor controlled with Siemens drives and interfaced with a Siemens PLC with a control loop rate of 0.04s. Trolley, hoist and slew positions were measured with rotary encoders on the motor shafts. Payload swing in both the radial and tangential directions was measured with an overhead camera attached to the trolley.

Each motion sequence was performed using four control methodologies: unshaped, ZV shaped, EI shaped, and with the CAID controller. The moves used in the studies were chosen to minimize the dependency of the system performance on the move itself. For example, a simple straight-line move using unshaped commands can “accidentally” cause zero residual vibration if the move distance happens to be the right value. These special cases can be avoided by testing multiple move distances. Each trajectory was also initiated from the same starting location to remove any bias from asymmetries in the operational

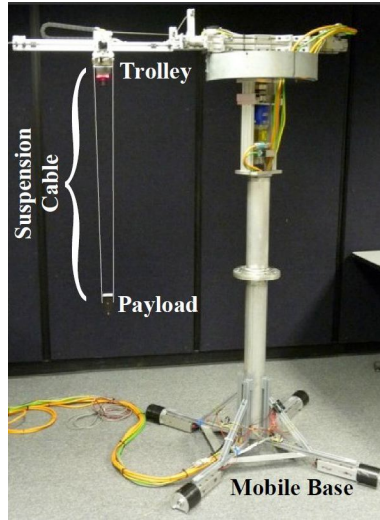


Figure 11. PORTABLE TOWER CRANE

workspace.

To excite the vibratory dynamics of the crane, each axis was operated near its performance limits. For the trolley axis these limits are a maximum velocity of $0.14 \frac{m}{s}$ and acceleration of $1.20 \frac{m}{s^2}$. For the slew axis, the velocity limit is $0.35 \frac{rad}{s}$ and the acceleration limit is $0.7 \frac{rad}{s^2}$. For the hoist axis, only a velocity limit of $0.13 \frac{m}{s}$ was included. Residual vibration results are expressed as the norm of the maximum radial and tangential residual vibrations.

Performance Comparisons

The first set of experiments assessed the performance of the CAID controller for point-to-point trolley motions. Table 2 shows the results for both short ($\Delta D = 0.21m$) and long ($\Delta D = 0.43m$) trolley motions. Both the ZV and CAID algorithms result in nearly the same move time, while the EI shaper takes significantly longer. All controllers, however, have a longer execution time than the unshaped case. Relative to the unshaped case, all the controllers result in drastic improvements in residual vibration. Contrary to the simulation results, the ZV shaper outperforms the CAID controller for this specific motion because the required CAID trajectory was partially unrealizable using the physical system, due primarily to the relatively low sampling frequency.

When slew axis motion is introduced, the CAID algorithm shows drastic improvements in performance over both the ZV and EI shapers. As expected, the CAID algorithm compensates for centripetal acceleration generated by the slewing motion resulting in decreased residual vibration when compared to the other command generation methods.

When the crane executes a trajectory using all three axes, the ZV and CAID speeds are comparable. However, the residual vibration of the CAID response more closely resembles that of the EI shaper. Thus, the CAID controller exhibits the speed of a ZV shaper with accommodation for variation in system parameters

Table 2. POINT-TO-POINT MOTIONS

<i>Move (m)(m)(°)</i>			<i>Move Time (s)</i>				<i>Res. Vib. (°)</i>			
ΔD	ΔR	ΔS	US	ZV	EI	CAID	US	ZV	EI	CAID
<i>Trolley Only</i>										
0.21	0	0	1.68	2.76	3.76	2.92	1.96	0.11	0.22	0.29
0.43	0	0	3.28	4.28	5.32	4.20	2.66	0.14	0.30	0.20
<i>Trolley + Slew</i>										
0.21	0	45	3.32	4.44	5.36	4.44	3.56	0.53	0.40	0.11
0.43	0	90	5.24	6.24	7.08	6.04	2.29	0.74	0.35	0.10
<i>Trolley + Hoist + Slew</i>										
0.21	0.61	90	5.16	6.08	7.16	6.20	2.69	0.94	0.41	0.45
0.43	1.22	180	9.72	10.70	11.70	10.80	1.94	0.82	0.27	0.35

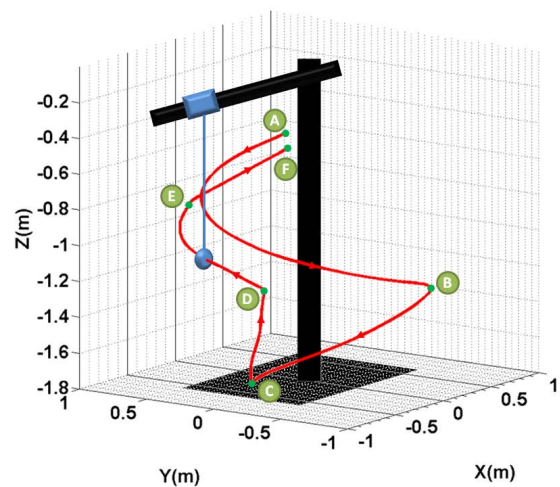


Figure 12. MULTI-WAYPOINT TRAJECTORY

like an EI shaper.

When a comparison is drawn between each of the techniques it is apparent that the CAID method provides a good combination of both speed and vibration reduction. ZV shaping results in comparably fast motions, but with increased residual vibrations when the nonlinearities become important. EI shaping creates trajectories with low residual vibration amplitudes for a wide range of conditions, but at the cost of slower operation.

A series of tests using a trajectory with 6 way-points was also executed. The specific trajectory is illustrated in Figure 12. It consists of 5 separate coordinated trajectories exercising all three axes. At each way-point the payload paused momentarily before continuing to the next location using the fastest possible trajectory.

Table 3. MULIT-WAYPOINT TRAJECTORY

<i>Move Time (s)</i>			<i>Res. Vib. (°)</i>		
ZV	EI	CAID	ZV	EI	CAID
32.6	36.7	33.5	4.93	1.07	1.08

The results using this complex trajectory are listed in Table 3. While the ZV shaper executes the trajectory in the shortest time, it also results in almost 5 degrees of residual vibration compared to only 1 degree for both the EI shaper and CAID controller. The EI shaper takes approximately 10% longer to complete the sequence of moves. These results indicate that the CAID method is the best approach for these preplanned complex trajectories.

Robustness Comparisons

Often the parameters of a system cannot be accurately estimated or they are unmeasurable. Thus, it is important to exhibit robustness to parameter errors, such as an incorrect hoist length. To evaluate robustness, several tests were performed to examine the performance of the CAID method relative to both the ZV and the EI shapers when modeling errors existed.

When the jib of the tower crane slews, centripetal acceleration causes radial deflection, the magnitude of which is proportional to the slew rate squared and the trolley position. Therefore, if the trolley position were recorded incorrectly and used to design the CAID trajectory, it would compensate incorrectly for the centripetal acceleration, causing errors in the response and residual vibration.

Table 4 summarizes the responses for several tests that include modeling errors of 44 – 90% in the trolley position and 24 – 56% in the hoist length. It is obvious that when the incorrect trolley position is used, the CAID residual vibration amplitudes are greater than any of the previous tests without parameter error. However, they are approximately the same as the ZV shaper results in magnitude.

As the length of the pendulum varies, the natural frequency changes, as previously described. The CAID method, like the ZV shaper, essentially seeks to cancel the resonant system poles by placing zeros over them. If the natural frequencies are identified incorrectly, then the cancellation will be imperfect. This results in trajectory error and residual vibration, as shown in Table 4. Conversely, the EI shaper suppresses vibrations over a large range of natural frequencies.

DISCUSSION

The flatness property provides a powerful framework for the generation of efficient commands for flexible motions systems, especially in the case of systems with nonlinear coupling between motion axes. Provided the desired trajectories are known before motion is initiated, and meet the continuity criteria outlined, the parameterization of the system in terms of the flat

Table 4. ROBUSTNESS TESTS

		<i>Ideal</i>	<i>Actual</i>	<i>Move</i>	<i>Res. Vib. (°)</i>		
<i>Slew w/Incorrect Trolley Pos.</i>							
D_{ideal}	D_{actual}	Slew	ZV	EI	CAID		
0.48	0.91	90	0.46	0.44	0.47		
0.48	0.69	90	0.50	0.32	0.50		
<i>Trolley w/Incorrect Hoist Length</i>							
R_{ideal}	R_{actual}	Trolley	ZV	EI	CAID		
1.09	1.70	0.43	0.36	0.17	0.34		
1.09	1.35	0.43	0.55	0.08	0.58		
<i>Slew w/Incorrect Hoist Length</i>							
R_{ideal}	R_{actual}	Slew	ZV	EI	CAID		
1.09	1.70	90	1.73	0.32	1.51		
1.09	1.35	90	0.91	0.19	0.84		

outputs provides a closed-form solution to the inverse dynamics problem. However, no guarantee exists that the commands produced will satisfy the constraints imposed by the physical system. The method must check the desired commands for limit violations, and selectively reduce the performance objectives of the desired trajectory until the generated commands meet the system limitations.

In both the simulated and experimental responses, the CAID controller provided smooth, low-vibration paths for a tower crane with move times comparable to a ZV shaper. Robustness of the proposed scheme to variations in system parameters was shown to be similar to that of a EI shaper. However, when system measurements are inaccurate or unavailable, ZV shaper like robustness properties are observed. This indicates that when trajectories are designed using inaccurate system values, extraneous residual and transient vibration will likely occur. However, this level of vibration will still be a significant improvement relative to the unshaped case. If parameters are particularly uncertain more robust techniques like EI shapers should be employed, but if parameters are known but change quickly, the flatness-based method is an excellent choice.

One significant drawback to the proposed approach is the requirement of C^4 desired trajectories. This requires predetermined start and end locations, and restricts its application to only autonomous or semi-autonomous operation where the trajectory is known before motion is initiated.

CONCLUSIONS

Using a trajectory-generation strategy based on the property of differential flatness for nonlinear systems, a series of simula-

tions and experiments were performed to assess the effectiveness and practicality of the proposed method. Guidelines for the creation of these trajectories were outlined, resulting in fast trajectories for realistic systems with performance constraints. Comparisons to standard input-shaping techniques were made indicating the flatness-based approach results in a good trade off between residual vibration and response time.

FUTURE WORK

While cranes are an excellent example of flexible motion systems, we believe that this approach could be applied to other prevalent systems where inherent flexibility necessitates the generation of trajectories that reduce vibrations. One such example is that of robot manipulators where workspace and performance size are sacrificed for the sake of rigidity. By enabling vibration-free motion with changing system dynamics, the utility of these systems could be improved by enabling lighter weight, higher performance manipulators.

Also outstanding is a closed form method for generating jerk limited trajectories that satisfy the criteria for the flatness based method, namely C^4 and satisfying the necessary boundary conditions. Numerical improvements could allow application on embedded systems to generate trajectories for achieving identified goal states in real time. For example, for use in pick-and-place operations.

ACKNOWLEDGEMENTS

The authors would like to thank Siemens Industrial Automation for their support of this work.

REFERENCES

- [1] S. P. Bhat and D. K. Miu. Precise point-to-point positioning control of flexible structures. *ASME Journal of Dynamic Systems Measurement and Control*, 112(4):667–674, 1990.
- [2] D. Blackburn, W. Singhose, J. Kitchen, V. Patrangenaru, J. Lawrence, Tatsuaki Kamoi, and Ayako Taura. Command shaping for nonlinear crane dynamics. *Journal of Vibration and Control*, 16(477):25, 2010.
- [3] David Blackburn, Jason Lawrence, Jon Danielson, William Singhose, Tatsuaki Kamoi, and Ayako Taura. Radial-motion assisted command shapers for nonlinear tower crane rotational slewing. *Control Engineering Practice*, 18, 2010.
- [4] W. Blajer and K. Kolodziejczyk. Motion planning and control of gantry cranes in cluttered work environment. *IET Control Theory Appl.*, 1(5), 2007.
- [5] Alessandro De Luca and Wayne J. Book. Robots with flexible elements. *Springer Handbook of Robotics*, pgs. 287–319. Springer, Berlin, 2008.
- [6] M. Fliess, J. Levine, P. Martin, and P. Rouchon. Flatness and defect of nonlinear systems: Introductory theory and examples. Tech. report, Ministere del Education Nationale, 1994.
- [7] M. Fliess, J. Levine, and P. Rouchon. A simplified approach of crane control via a generalized state-space model. *30th Conference on Decision and Control*. Brighton, England, 1991.
- [8] ShihChung Kang and Eduardo Miranda. Physics based model for simulating the dynamics of tower cranes. *International Conference on Computing in Civil and Building Engineering*. Weimar, Germany, 2004.
- [9] Balint Kiss, Jean Levine, and Philippe Mullhaupt. Modeling, flatness and simulation of a class of cranes. *Periodica Polytechnica*, 43(3):10, 1999.
- [10] Dong Soo Kwon and Wayne J. Book. A time domain inverse dynamic tracking control of a single-link flexible manipulator. *Journal of Dynamic Systems, Measurement, and Control*, 116(2), 1994.
- [11] David P. Magee and Wayne J. Book. Optimal filtering to minimize the elastic behavior in serial link manipulators. *American Control Conference*. Philadelphia, Pennsylvania, 1998.
- [12] Ehsan Maleki, Brice Pridgen, Jing Qi Xiong, and William Singhose. Dynamic analysis and control of a portable cherrypicker. *Dynamic Systems and Controls Conference*. Boston, Massachusetts, 2010.
- [13] Ali Mansour and Housseem Jerbi. An exact differential flatness control for a non minimum phase model of an inverted pendulum. *Third Asia Conference on Modelling and Simulation*. Bundang, Indonesia, 2009.
- [14] A. Piazzoli and A. Visioli. Optimal dynamic-inversion-based control of an overhead crane. *IEE Proc.-Control Theory Appl.*, 149(5), 2002.
- [15] N. C. Singer and W. P. Seering. Preshaping command inputs to reduce system vibration. *Journal of Dynamic Systems, Measurement, and Control*, 93(101):1971–1979, 1990.
- [16] W. Singhose, W. P. Seering, and N. C. Singer. Residual vibration reduction using vector diagrams to generate shaped inputs. *ASME Journal of Mechanical Design*, 116(June):654–659, 1994.
- [17] William Singhose. Command shaping for flexible systems: A review of the first 50 years. *Int. J. of Precision Engineering and Manufacturing*, 10(153-168):153–168, 2009.
- [18] William Singhose, R. Eloundou, and Jason Lawrence. Command generation for flexible systems by input shaping and command smoothing. *Journal of Guidance, Control, and Dynamics*, 33(6), 2010.
- [19] William Singhose and Warren Seering. *Command Generation for Dynamic Systems*. ISBN 978-0-9842210-0-4, 2009.
- [20] O. J. M. Smith. *Feedback Control Systems*. McGraw-Hill Book Co., New York, 1958.
- [21] Motoji Yamamoto, Noritaka Yanai, and Akira Mohri. Inverse dynamics and control of crane-type manipulator. *International Conference on Intelligent Robots and Systems*. Kyongju, 1999.